

The author is grateful to Prof. A. I. Leipunskii for continued interest in the work.

<sup>1</sup>Hamermesh, Hamermesh and Wattenberg, Phys. Rev. **76**, 611 (1949).

<sup>2</sup>E. P. Meiners, Phys. Rev. **76**, 259 (1949).

<sup>3</sup>A. Wattenberg, Phys. Rev. **71**, 497 (1947).

<sup>4</sup>D. J. Hughes and C. Egger, Phys. Rev. **72**, 902 (1947).

<sup>5</sup>R. Culp and B. Hamermesh, Phys. Rev. **93**, 1025 (1954).

<sup>6</sup>Dzhelepov, Zhukovsky, Nedovesov, Uchevatkin and Chumin, Nucl. Phys. **2**, 408 (1956).

<sup>7</sup>B. Hamermesh and C. Kimball, Phys. Rev. **90**, 1063 (1953).

<sup>8</sup>A. O. Hanson and J. L. McKibben, Phys. Rev. **72**, 673 (1947).

<sup>9</sup>Barschall, Battat, Bright, Graves, Jorgensen and Manley, Phys. Rev. **72**, 881 (1947).

<sup>10</sup>G. N. Lovchikova, Атомная энергия (Atomic Energy) **2**, 174 (1957).

<sup>11</sup>M. Walt and H. H. Barschall, Phys. Rev. **93**, 1062 (1954).

<sup>12</sup>M. Walt, P/588, Proceedings of the International Conference on the Peaceful Uses of Atomic Energy, Geneva, 1956, Vol. 2, p. 18.

<sup>13</sup>H. Feshbach and V. F. Weisskopf, Phys. Rev. **76**, 1550 (1949).

<sup>14</sup>D. J. Hughes and J. A. Harvey, Neutron Cross Sections, New York, 1955.

<sup>15</sup>H. C. Martin and R. F. Taschek, Phys. Rev. **89**, 1302 (1953).

<sup>16</sup>V. Hummel and B. Hamermesh, Phys. Rev. **82**, 67 (1951).

<sup>17</sup>R. L. Henkel and H. H. Barschall, Phys. Rev. **80**, 145 (1950).

<sup>18</sup>L. E. Beghian and H. H. Halban, Nature **163**, 366 (1949).

Translated by M. Hamermesh

114

## ELECTRON LOSS AND CAPTURE IN COLLISIONS BETWEEN FAST HYDROGEN ATOMS AND MOLECULES OF GASES

Ia. M. FOGEL', V. A. ANKUDINOV, D. V. PILIPENKO and N. V. TOPOLIA

Physico-Technical Institute, Academy of Sciences, Ukrainian S.S.R.

Submitted to JETP editor September 30, 1957

J. Exptl. Theoret. Phys. (U.S.S.R.) **34**, 579-592 (March, 1958)

The cross sections for capture and loss of electrons in single collisions of 5-keV to 40-keV hydrogen atoms with He, Ne, Ar, Kr and Xe atoms and with H<sub>2</sub>, N<sub>2</sub> and O<sub>2</sub> molecules are measured by a mass-spectrometric method.

### INTRODUCTION

THE passage of fast neutral particles through a substance is accompanied by processes of electron capture and loss as the particles collide with atoms of the substance. The first of these processes can occur only if the neutral particle possesses positive electron affinity. As a result of electron capture and loss a neutral beam which has traversed a layer of matter will upon emerging contain singly charged negative ions and positive ions of various charge multiplicities in addition to neutral particles. A beam of hydrogen atoms, each of which can capture or lose only a single electron, will upon emerging

include negative hydrogen ions, hydrogen atoms and protons. For thin layers of matter permitting only single collisions the composition of the emerging beam will be determined by the cross sections for electron capture ( $\sigma_{0-1}$ ) and loss ( $\sigma_{01}$ ) by hydrogen atoms ( $\sigma_{ik}$  is the cross section for a process whereby a particle with charge  $ie$  is transformed into a particle with charge  $ke$ ). For thicker layers, where multiple collisions begin to play a part, the composition of the emerging beam is determined not only by the two cross sections already mentioned but also by  $\sigma_{10}$ ,  $\sigma_{-10}$ ,  $\sigma_{1-1}$  and  $\sigma_{-11}$ . Of these six cross sections for a hydrogen beam the cross section  $\sigma_{10}$  for the capture of a single elec-

tron by protons has been most completely investigated.<sup>1-8</sup>

The most important of the cross sections that determine the composition of a hydrogen beam is  $\sigma_{10}$ , since it determines the attenuation of a proton beam in its passage through matter. It is also possible to compare the experimental values of  $\sigma_{10}$  for protons in hydrogen and helium with a number of theoretical calculations.<sup>9-14</sup>

There have been several investigations to determine the cross sections  $\sigma_{01}$  and  $\sigma_{-10}$  for electron loss by hydrogen atoms<sup>9,15,16</sup> and by negative hydrogen ions,<sup>4,5,7,16</sup> respectively. The cross sections  $\sigma_{1-1}$  and  $\sigma_{-11}$  for the capture and loss of two electrons by protons and negative hydrogen ions, respectively, have also been measured.<sup>17,18</sup> There has been no direct measurement of the cross section  $\sigma_{0-1}$  for electron capture by hydrogen atoms. In Ref. 16 this cross section was calculated from measurements of  $\sigma_{-10}$  and  $(N^-/N^0)_p$ , which is the ratio of the negatively charged component to the neutral component in a beam of equilibrium composition assuming  $\sigma_{1-1} = \sigma_{-11} = 0$ .

The capture of electrons by neutral atoms is of considerable interest because in this case the electron is bound at the electron affinity level. There may be a definite correlation between the electron affinity of atoms that capture electrons and  $\sigma_{0-1}$ . Such a correlation would make it possible to determine the electron affinity, which cannot be measured easily. It is also of interest to determine to what extent electron capture by neutral particles satisfies Massey's adiabatic criterion. It should be noted that the theoretical calculation of  $\sigma_{0-1}$  is somewhat simplified by the absence of excited levels in many negative ions, as a result of which electrons are captured only at the ground level.

Recent investigations<sup>19-21</sup> have shown that the most promising method of producing a strong negative ion beam is the conversion of positive ions into negative ions by sending them through a layer

of matter. The negative ions appear both through single processes  $I^+ \rightarrow I^-$  (capture of two electrons by a positive ion in a single collision) and in stages:  $I^+ \rightarrow I^0$  and  $I^0 \rightarrow I^-$ . Hence for the purpose of calculating the negative ion content of the emerging beam  $\sigma_{0-1}$  must be known in addition to other cross sections. It should also be noted that knowledge of the cross sections for all inelastic interactions between hydrogen particles and gas molecules will make it possible to improve the calculations of energy losses by protons of moderate energies ( $E \approx E_0$ ) passing through gases.<sup>22</sup>

The foregoing considerations induced us to develop the apparatus and experimental procedure for the measurement of  $\sigma_{0-1}$ . As the first part of our program of measuring  $\sigma_{0-1}$  for H, C, O, Cl and F atoms, the present article gives measurements of  $\sigma_{0-1}$  for hydrogen atoms colliding with He, Ne, Ar, Kr and Xe atoms and H<sub>2</sub>, N<sub>2</sub> and O<sub>2</sub> molecules. Since our procedure enabled us to measure both  $\sigma_{0-1}$  and also  $\sigma_{01}$  for electron loss by hydrogen atoms, the data for the latter are also given.

## APPARATUS AND EXPERIMENTAL PROCEDURE

To obtain a beam of hydrogen atoms we neutralized protons by sending them through a mercury vapor target, which we had previously used<sup>18,19</sup> to produce a beam of negative hydrogen ions. Figure 1 is a diagram of the apparatus used in the present experiments. A hydrogen ion beam came from an ion gun which consisted of a high-frequency ion source 1 of the Reifenschweiler type,<sup>23</sup> a three-electrode lens 2 and an accelerating tube 3. The electrostatic corrector 4 was used to correct the direction of the ion beam. A monoenergetic proton beam which was selected by the magnetic mass monochromator 5 entered the mercury vapor target chamber 6, which was described in Ref. 19. The beam emerging from the mercury vapor contained protons and negative hydrogen ions in addition to hydrogen atoms. A second magnetic ana-

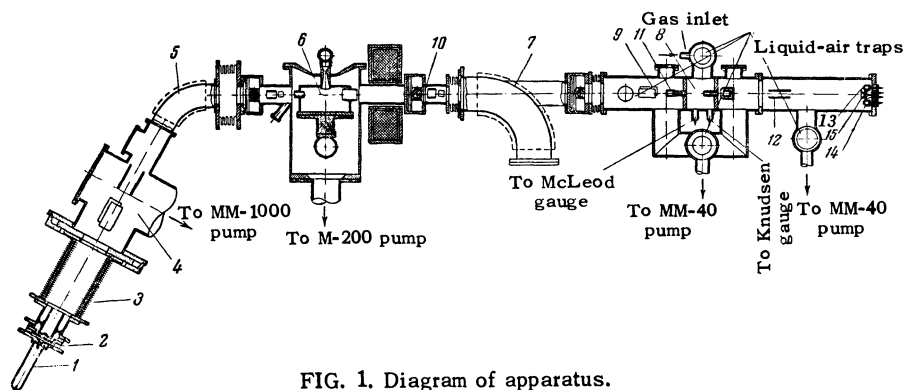


FIG. 1. Diagram of apparatus.

lyzer 7 separated the charged and neutral particles. A small admixture of charged particles in the hydrogen atom beam resulted from collisions of atoms with residual gas molecules along the path from the magnetic analyzer to the entrance diaphragm of the collision chamber 8. These charged particles were removed from the neutral beam by the plane condenser 9 placed before the entrance to the collision chamber. The neutral beam was collimated by two diaphragms 10 and 11. One of these, of 3-mm diameter aperture, was placed directly behind the mercury vapor target; the second, of 2 mm diameter, was aligned axially in front of the entrance tube of the collision chamber. This tube was 5 mm in diameter and 50 mm long. The beam emerged from the collision chamber through a tube of the same length and diameter. The distance from the exit plane of the entrance tube to the entrance plane of the exit tube was 50 mm. The equivalent current of the hydrogen atom beam entering the collision chamber was between  $10^{-9}$  and  $4 \times 10^{-8}$  amperes. The beam intensity was enhanced with increasing energy of the hydrogen atoms because of better focusing of the proton beam at higher energies. To obtain 5-keV H atoms we used the process  $H_3^+ \rightarrow H_1$  (a beam of 15-keV  $H_3^+$  ions was directed at the mercury vapor target) since at 5 keV the proton beam was poorly focused on the target by the ion gun.

The beam emerging from the collision chamber was separated into neutral, positive, and negative components by the electric field of the plane condenser 12, which consisted of plates 80 mm long separated by 24 mm. The currents of the charged components were measured by means of Faraday cylinders 13 and 14. The  $H_1^-$  current was measured by an EMU-3 vacuum tube electrometer with a sensitivity of  $10^{-14}$  amperes per division; the proton current was measured by a string electrometer with a sensitivity of  $10^{-12}$  amperes per division. Vacuum thermocouple 15 was used to measure the intensity of the neutral component. The thermoelectric power of the thermocouple was measured by an M107/3 mirror galvanometer with a sensitivity  $2 \times 10^{-8}$  volts per division.

The pressure of the gas which entered the collision chamber was measured by a Knudsen gauge calibrated against a McLeod gauge. The residual gas pressure in the chamber was  $2 \times 10^{-5}$  mm Hg.

The cross sections  $\sigma_{0-1}$  and  $\sigma_{01}$  were determined by the mass-spectrometric method which was described in detail in Refs. 17, 18, 24 and 25. This method investigates the dependence of the ratios  $N^-/N^0$  and  $N^+/N^0$  on the gas pressure in the collision chamber.  $N^-/N^0$  and  $N^+/N^0$  are the

ratios of the number of negative hydrogen ions and the number of protons, respectively, to the number of hydrogen atoms in the beam passing through gas in the collision chamber. Since different detectors were used to measure the intensities of the charged components and the neutral component of the beam, the vacuum thermocouple used to detect the neutral component had to measure the absolute intensity of the neutral beam.

For absolute measurements of the neutral beam intensity we used a vacuum thermocouple that was essentially similar to the thermocouple described in Ref. 21. The thermocouple was calibrated by means of a proton beam; simultaneous measurement was performed of the proton current strength reaching the receiver of the thermocouple and the thermoelectric power generated in the junction. The calibration factor was determined for all energies at which we were to measure the cross sections of interest.

It was essential for the correctness of the measurements of  $N^-/N^0$  and  $N^+/N^0$  and thus for the correctness of  $\sigma_{0-1}$  and  $\sigma_{01}$  that the entire beam of neutral particles should reach the thermocouple receiver, i.e., the beam axis had to pass through the center of the diaphragm aperture and the diameter of the beam had to be smaller than the diameter of the aperture. Otherwise the measured ratios  $N^-/N^0$  and  $N^+/N^0$  are too large, because the 14 mm diameter of the openings of the Faraday cups was large enough to admit the charged components of the beam entirely.

In order to verify that the entire neutral beam was reaching the thermocouple, a diaphragm with variable aperture was placed in front of the thermocouple for the purpose of determining the beam diameter. This diameter was 4.5 mm for beam energies of 5, 10 and 20 keV while the thermocouple aperture was 6 mm in diameter.

The neutral beam produced by the  $H_1 \rightarrow H_1^0$  conversion from 10 to 40 keV was intense enough to cause deflections of not less than 20 to 30 divisions of the galvanometer used to measure the thermoelectric power of the thermocouple. However, at 5-keV beam energy the deflection was still very small, both because of the reduced particle energy and because at 5 keV the ion gun achieved poor focusing of the proton beam on the mercury vapor target.

The conversion  $H_3^+ \rightarrow H_1^0$  can be used to produce a beam of 5-keV hydrogen atoms. A beam of 15-keV  $H_3^+$  ions is properly focused on the mercury-vapor target by the ion gun. On the other hand, the conversion coefficient of molecular hydrogen ions transformed into atoms is larger than for protons,

as we established in our investigation of the conversion of positive to negative hydrogen ions in a mercury-vapor target.<sup>19</sup> In earlier work (Ref. 18) we used the  $H_3^+ \rightarrow H_1^-$  conversion to produce a beam of low-energy  $H_1^-$  ions. But in using  $H_3^+ \rightarrow H_1^0$  to produce a beam of hydrogen atoms, a difficulty is encountered which is absent when the dissociation of molecular ions is used to obtain negative ions. This difficulty lies in the fact that as a result of the dissociation of  $H_3^+$  ions with energy  $E$ , in addition to  $H_1^0$  atoms with energy  $\frac{1}{3}E$ ,  $H_2^0$  molecules with energy  $\frac{2}{3}E$  can be produced ( $H_3^0$  is unstable). Only when the number of  $H_2^0$  molecules in the neutral beam emerging from the mercury-vapor target is small compared with the number of  $H_1^0$  atoms can this beam be used to measure the cross sections of interest. It is thus necessary to have some method of determining the relative content of  $H_1^0$  and  $H_2^0$  in the neutral beam. The neutral beam produced after passage of  $H_3^+$  ions through the mercury-vapor target traversed a collision chamber filled with argon at  $2 \times 10^{-4}$  mm Hg. Because of the loss of electrons by  $H_1^0$  and  $H_2^0$  through collisions with argon atoms the beam emerging from the collision chamber had to contain particles of  $H_1^+$  with the energy  $\frac{1}{3}E$  and  $H_2^+$  with the energy  $\frac{2}{3}E$ ,  $E$  being the energy of the  $H_3^+$  ions striking the mercury-vapor target. The emerging beam was found to contain positively charged particles with the energies  $\frac{1}{3}E$  and  $\frac{2}{3}E$ . These are evidently the ions  $H_1^+$  and  $H_2^+$  that result from collisions of  $H_1^0$  and  $H_2^0$  with argon atoms, with the loss of electrons. This provides confirmation of the hypothesis that the neutral beam produced by passing  $H_3^+$  ions through a mercury vapor target consists of  $H_1^0$  and  $H_2^0$ .

It is evident that the relative numbers of  $H_1^0$  and  $H_2^0$  in the neutral beam must depend on the thickness of the mercury-vapor target. Specifically, we cannot exclude the possibility of complete dissociation of the molecules into atoms in a target of sufficient thickness. In order to determine whether this occurs we investigated the relation between the  $H_1^+$  and  $H_2^+$  currents in the beam after the neutral beam had traversed the argon-filled chamber, and the thickness of the mercury vapor target. The target thickness was varied by changing the boiler temperature (see Ref. 26). Figure 2 shows  $I_{H_1^+}$  and  $I_{H_2^+}$  as functions of the boiler temperature. It can be seen that  $I_{H_1^+}$  and  $I_{H_2^+}$  pass through a maximum and begin to diminish with further increase of the boiler temperature; this results from scattering in the mercury vapor jet. However,  $I_{H_2^+}$  diminishes much more rapidly than  $I_{H_1^+}$ ; this apparently results from increased dissociation of

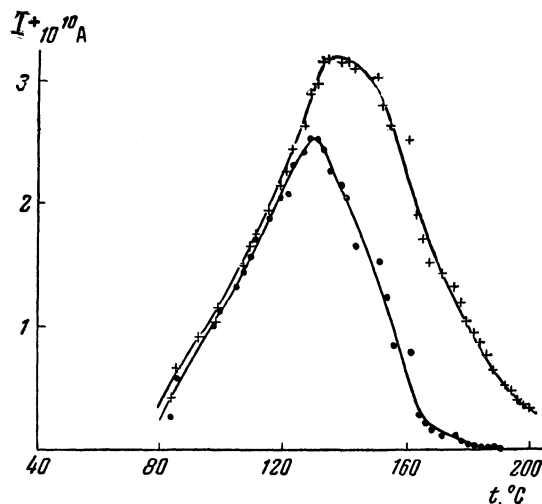


FIG. 2. The Currents  $I_{H_1^+}$  and  $I_{H_2^+}$  as functions of the boiler temperature: + - for  $H_1^+$ ; • - for  $H_2^+$ .

molecules to form atoms as the target thickness is increased. At  $t_{\text{boiler}} \approx 190^\circ\text{C}$  we have  $I_{H_1^+} = 6.3 \times 10^{-11}$  amp while  $I_{H_2^+} < 2 \times 10^{-13}$  amp. It thus follows that when the target thickness corresponds to  $t_{\text{boiler}} = 190^\circ\text{C}$  the neutral beam that results from passage of  $H_3^+$  ions through the target is practically completely atomic in character. This is also confirmed by the fact that the cross sections  $\sigma_{0-1}$  and  $\sigma_{01}$  as measured with a neutral beam from 10-keV protons and with a neutral beam from 30-keV  $H_3^+$  ions were identical within the limits of experimental error. The measurements of  $\sigma_{0-1}$  and  $\sigma_{01}$  with 5-keV neutral beams obtained from  $H_3^+ \rightarrow H_1^0$  were subsequently performed at a boiler temperature of  $200^\circ\text{C}$ .

There are inherent systematic errors in the mass-spectrometric method which we used to measure  $\sigma_{0-1}$  and  $\sigma_{01}$ . These result from: (a) the influence of the pressure and composition of the residual gas in the apparatus on the magnitudes of the measured cross sections;<sup>25</sup> (b) unequal scattering of protons, atoms and negative hydrogen ions in the collision chamber; (c) unequal attenuation of the beams of protons, atoms and ions on their path from the collision chamber to the vacuum thermocouple and Faraday cups of the analyzer.

By investigating the dependence of  $\sigma_{0-1}$  and  $\sigma_{01}$  on  $(N^-/N^0)_f$  and  $(N^+/N^0)_f$ \* we have shown that the error due to residual gas in the path of the beam is small and within the limits of experimental error. In order to determine the influence of unequal scattering in the collision chamber we measured  $\sigma_{0-1}$  and  $\sigma_{01}$  with an aperture of 2 mm

\* $(N^-/N^0)_f$  and  $(N^+/N^0)_f$  are the values of  $N^-/N^0$  and  $N^+/N^0$  when no gas is admitted into the collision chamber.

diameter behind the collision-chamber outlet and axially aligned with the exit tube, as well as in the absence of this aperture.\* This aperture reduced to one sixth the solid angle of emission of the particles leaving the collision chamber. Measurements were performed at beam energies of 15 and 30 keV in He and Kr. Identical values within the limits of experimental error were found for  $\sigma_{0-1}$  and  $\sigma_{01}$  with and without the use of the diaphragm aperture behind the exit tube. Thus the scattering of particles in the collision chamber does not seriously affect the measurements. The correction for unequal attenuation of the separate beams in the analyzer does not exceed a few tenths of one per cent and is unimportant. Random errors amounted to  $\pm 20\%$  for  $\sigma_{0-1}$  and  $\pm 15\%$  for  $\sigma_{01}$ .

The energy of the hydrogen atoms was determined from the sum of the potential differences across the ion source and accelerating tube, which were measured by electrostatic voltmeters calibrated against a resistance voltmeter. As we have shown in Ref. 18, the energy loss of the protons in traversing the mercury vapor target is very small. There was an error of  $\pm 3\%$  in the measurement of the hydrogen atom energy.

## RESULTS AND DISCUSSION

We measured the cross sections for electron capture and loss in collisions of hydrogen atoms at 5 to 40 keV with He, Ne, Ar, Kr and Xe atoms and H<sub>2</sub>, N<sub>2</sub> and O<sub>2</sub> molecules. The collision chamber was filled with hydrogen passed through a palladium barrier, spectrally pure helium, neon, krypton and xenon, oxygen with 0.9% impurity, argon with 0.3% impurity and nitrogen with 0.03% impurity.

Figures 3 and 4 show the cross sections  $\sigma_{0-1}$  and  $\sigma_{01}$  as functions of the hydrogen atom energy for atomic and molecular gases. The cross section at each energy was obtained by averaging two measurements, and was computed per gas particle, which in the case of the molecular gases means per gas molecule.

Figures 3 and 4 show that in the investigated energy range  $\sigma_{0-1}$  for H atoms in He, Ne, H<sub>2</sub>, N<sub>2</sub> and O<sub>2</sub> passes through a maximum, which with He occurs at 20 keV and with Ne<sub>2</sub>, H<sub>2</sub>, N<sub>2</sub> and O<sub>2</sub> at  $\sim 10$  keV. In Ar, Kr and Xe  $\sigma_{0-1}$  decreases monotonically with rising energy.  $\sigma_{0-1}$  varies

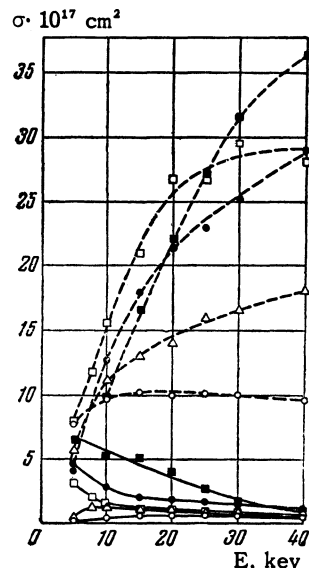


FIG. 3.  $\sigma_{0-1}$  (solid curves);  $\sigma_{01}$  (dashed curves).  $\circ$  - He,  $\Delta$  - Ne,  $\square$  - Ar,  $\bullet$  - Kr,  $\blacksquare$  - Xe.

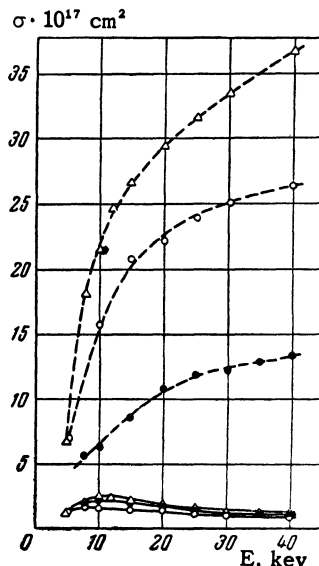


FIG. 4.  $\sigma_{0-1}$  (solid curves);  $\sigma_{01}$  (dashed curves).  $\bullet$  - H<sub>2</sub>,  $\circ$  - O<sub>2</sub>,  $\Delta$  - N<sub>2</sub>.

from  $2.4 \times 10^{-18} \text{ cm}^2$  (in He at 5 keV) to  $6.6 \times 10^{-17} \text{ cm}^2$  (in Xe at 5 keV). For the molecular gases  $\sigma_{0-1}$ , within the limits of error, does not depend on the kind of gas. For atomic gases  $\sigma_{0-1}$  is observed to depend on the kind of gas, especially at low energies.  $\sigma_{0-1}$  increases with the atomic number of the inert gas.

For all gases except He  $\sigma_{01}$  decreases with reduced energy of the H atoms. The maximum of  $\sigma_{01}$  for He occurs at 15 keV.  $\sigma_{01}$  varies from  $4.2 \times 10^{-17} \text{ cm}^2$  (in Kr at 5 keV) to  $3.7 \times 10^{-16} \text{ cm}^2$  (in Xe and N<sub>2</sub> at 40 keV).  $\sigma_{01}$  is about one order of magnitude larger than  $\sigma_{0-1}$ .

It is of interest to compare our results with

\*It is not desirable to have a diaphragm directly at the exit aperture of the exit tube since this would distort the pressure distribution in the tube and change the effective length of the collision chamber.

those obtained by other investigators. As mentioned in the introduction, there were no direct measurements of  $\sigma_{0-1}$ . For  $H_2$ ,  $N_2$ ,  $O_2$ , He, Ne and A it is possible to make a comparison with the values for  $\sigma_{0-1}$  calculated by Stier and Barnett<sup>16</sup> from measurements of  $\sigma_{-10}$  and  $(N^-/N^0)_p$  assuming small cross sections for two-electron transfers ( $\sigma_{1-1} = \sigma_{-11} = 0$ ). For  $H_2$   $\sigma_{0-1}$  was calculated by Whittier<sup>5</sup> using his own measurements of  $(N^-/N^+)_p$  and  $\sigma_{-10}$  and Bartels' measurements of  $(N^+/N^-)_p$ .

Our measurements of  $\sigma_{01}$  for  $H_2$ ,  $N_2$ ,  $O_2$ , He, Ne and A can be compared with those of Stier and Barnett.<sup>16</sup> Montague<sup>15</sup> also measured  $\sigma_{01}$  in  $H_2$ , but his data cover the energy range 45–329 keV, which is outside our energy range.\*  $\sigma_{01}$  was calculated theoretically for atomic hydrogen by Bates and Griffing<sup>28</sup> and for helium by Bates and Williamson.<sup>29</sup>

Figure 5 shows  $\sigma_{0-1}$  and  $\sigma_{01}$  as functions of energy for  $H_2$ ,  $N_2$ ,  $O_2$ , He, Ne and A; the values obtained in the present investigation are compared with those obtained by other writers.† The figures show that our values for  $\sigma_{0-1}$  are in good agreement with the calculations of Stier and Barnett, but that for  $H_2$  they differ somewhat from those computed by Whittier. The fact that these investigators calculated  $\sigma_{0-1}$  without taking account of two-electron transfers could not have introduced any considerable error; our measurements<sup>17,18</sup> have shown that the cross sections for such transfers are small compared with those for one-electron transfers.

Figure 5 shows that our values for  $\sigma_{01}$  are consistently lower than those measured by Stier and Barnett, although the curves have similar shapes. The beginning of Montague's curve (Fig. 5) is more consistent with our curve than with that of Stier and Barnett although the American authors all used the same method of neutral beam attenuation while our measurements were obtained by a mass-spectrometric method. When the values of  $\sigma_{0-1}$  and  $\sigma_{01}$  given by different writers are compared it must be kept in mind that the discrepancies may be caused by an admixture of excited metastable atoms in the neutral beam that enters the collision chamber. The percentage of metastable atoms in the neutral beam can differ in the various

\*Montague actually measured the sum  $\sigma_{01} + \sigma_{0-1}$ , but since  $\sigma_{01} \gg \sigma_{0-1}$  this sum differs very little from  $\sigma_{01}$ .

†Since other authors give the cross sections per gas atom our values for  $\sigma_{0-1}$  and  $\sigma_{01}$  in the case of the molecular gases which are given in Fig. 5 were obtained by halving the measurements.

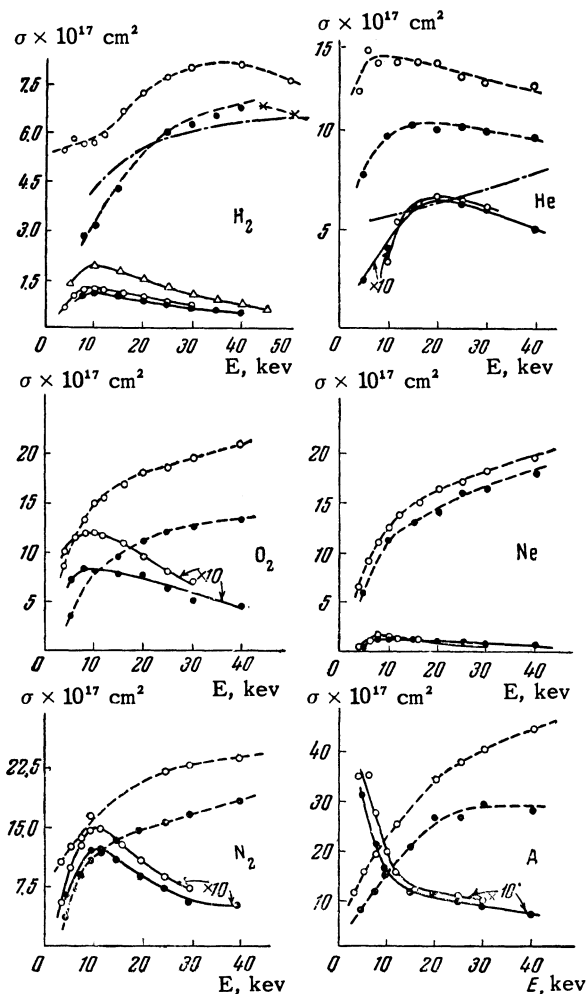


FIG. 5.  $\sigma_{0-1}$  (solid curves);  $\sigma_{01}$  (dashed curves);  $\sigma_{01}$  (dots and dashes) from Refs. 28 and 29. O — from Ref. 16; × — from Ref. 15; Δ — from Ref. 5; ● — our present data.

experiments depending on the experimental conditions (different targets for neutralizing the original charged beam, different distances between the target and collision chamber) and thus account for the discrepancies between the results.

The foregoing considerations provide no explanation of the discrepancy between the value of  $\sigma_{01}$  obtained in the present work and that of Stier and Barnett.<sup>16</sup> Although the hydrogen atom possesses a metastable  $2^2S_{1/2}$  state with a lifetime of the order of 0.1 sec, in both experiments the neutral beam before entering the collision chamber passed through the electric field of the condenser which removed charged particles. This field reduced the lifetime of the excited atoms to  $2 \times 10^{-8}$  sec, so that the neutral beam entered the collision chamber in an unexcited state.

A comparison of the experimental and theoretically computed values of  $\sigma_{01}$  (Fig. 5) shows that in the 5- to 40-keV energy range for hydrogen the

theoretical values are in good agreement with the experimental results obtained in the present work and by Montague. For helium there is considerable difference between the theoretical and experimental curves with regard to both magnitude and form. The experimental curves pass through a maximum at 10 – 12 kev, whereas the theoretical curve rises monotonically in this range.\*

In the comparison of theoretical with experimental results the following circumstances must be kept in mind.  $\sigma_{01}$  is computed theoretically for atomic hydrogen whereas the experiments are performed with molecular hydrogen. In the comparison it is therefore assumed that a molecule of hydrogen is equivalent to two atoms. In Refs. 28 and 29  $\sigma_{01}$  was calculated in a Born approximation; the values thus obtained should generally be valid for  $E \gg E_0$  ( $E_0 = 25$  kev, which is the energy at which the velocity of the hydrogen atom equals the orbital velocity of the electron). Indeed, for  $E > 100$  kev we find good agreement between theory and the experimental results of Stier and Barnett in the case of helium. For hydrogen the agreement is not so good but is still satisfactory (see Ref. 29). Thus the disagreement between theory and experiment for helium in the vicinity of  $E \approx E_0$  is not surprising, as the Born approximation is not generally applicable to this energy range. On the other hand, the good agreement between theory and experiment for hydrogen is evidence either that the experimental results for  $\sigma_{01}$  are inaccurate or that the Born approximation in this special instance is valid up to  $E \approx E_0$ . We know that the calculation of  $\sigma_{10}$  by the Born approximation for protons in hydrogen is in very good agreement with experiment up to energies of the order of  $E_0$ .<sup>14</sup> Jackson<sup>30</sup> has shown that this is not accidental but is associated with the fact that when the total interaction Hamiltonian is used for  $Z = Z' = 1$  (where  $Z$  and  $Z'$  are the atomic numbers of the incident and struck particle, respectively) the correction to the matrix element in the second Born approximation is zero. There may be a good theoretical reason for the applicability of the Born approximation to  $\sigma_{01}$  near  $E \sim E_0$  for hydrogen atoms in hydrogen.

As mentioned in the Introduction, the composition of a hydrogen beam that has passed through matter is determined by the six cross sections  $\sigma_{10}$ ,  $\sigma_{01}$ ,  $\sigma_{0-1}$ ,  $\sigma_{-10}$ ,  $\sigma_{1-1}$ ,  $\sigma_{-11}$ . For a beam in equilibrium we have<sup>17</sup>

$$\left(\frac{N^-}{N^+}\right)_p = \frac{\sigma_{10}\sigma_{0-1} + \sigma_{1-1}\sigma_{01} + \sigma_{1-1}\sigma_{0-1}}{\sigma_{01}\sigma_{-10} + \sigma_{-11}\sigma_{01} + \sigma_{-11}\sigma_{0-1}}. \quad (1)$$

For a hydrogen target there have been determined in our laboratory  $\sigma_{10}$ ,<sup>6</sup>  $\sigma_{1-1}$ ,<sup>17</sup>  $\sigma_{-11}$ ,<sup>18</sup>  $\sigma_{01}$  and  $\sigma_{0-1}$  (the present work), and also  $(N^-/N^+)_p$ .<sup>\*</sup> Substituting these results in Eq. (1), we can derive  $\sigma_{-10}$  and compare this result with the measurements in Refs. 5 and 16. Figure 6 shows good agreement between our calculation for  $\sigma_{-10}$  and the results in Ref. 5 but somewhat greater divergence from the results in Ref. 16. Considering the cumulative error in the calculation of  $\sigma_{-10}$  and the appreciable error in the measurements of  $\sigma_{-10}$  in Ref. 16, the discrepancy is within the limits of experimental error.

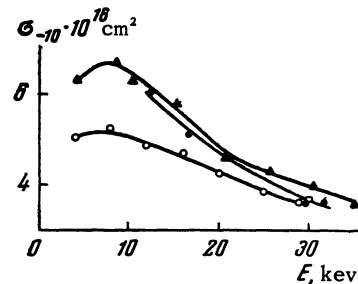


FIG. 6. ▲— data from Ref. 5; ○— data from Ref. 16; ●— computed from Eq. (2); □— computed from Eq. (5).

By using the solutions of the differential equations that determine the composition of a hydrogen beam [see Eq. (3) of Ref. 17], it can be shown that at very low gas pressures in the collision chamber the following relation exists between  $N^+/N^-$  and pressure:

$$N^+/N^- = \alpha p + \Omega p^2, \quad (2)$$

where

$$\alpha = \sigma_{-11} L / kT \quad (3)$$

$$\Omega = \frac{1}{2} [\sigma_{-10}\sigma_{01} + \sigma_{-11}(\sigma_{-10} + \sigma_{-11} - \sigma_{10} - \sigma_{1-1})] (L/kT)^2. \quad (4)$$

Experiment shows that the beginning of the curve  $N^+/N^- = f(p)$  always satisfies Eq. (2). By applying the method of least squares to the experimental results, we can determine  $\Omega$  and then  $\sigma_{-10}$  from Eq. (4). We have plotted the curve  $N^+/N^- = f(p)$  for  $H_2$  and  $H_1^-$  ions of 30-kev energy† and used the foregoing method to compute  $\sigma_{-10}$ . This value

\*The results given in Ref. 17 for  $(N^-/N^+)_p$  in  $H_2$  have been checked with our apparatus. Our results were 20% higher than those of Ref. 17 and were in good agreement with Whittier<sup>5</sup> and Stier and Barnett.<sup>16</sup> These results have been used for the computation of  $\sigma_{-10}$  through Eq. (2).

†For this purpose we used the apparatus described in Ref. 18.

\*The theoretical curve reaches its maximum at 60 kev (Ref. 29).

of  $\sigma_{-10}$  in Fig. 6 is in good agreement with both the value calculated for an equilibrium beam and with experimental measurements.

The pressure dependence of  $N^-/N^+$  over the entire pressure range as far as the equilibrium point is given [see Eq. (3) of Ref. 17] by the formula

$$\frac{N^-}{N^+} = \frac{a_0 + a_1 \exp\{-(r_1 L / kT) p\} + a_2 \exp\{-(r_2 L / kT) p\}}{b_0 + b_1 \exp\{-(r_1 L / kT) p\} + b_2 \exp\{-(r_2 L / kT) p\}}, \quad (5)$$

where  $r_1$ ,  $r_2$ ,  $a_0$ ,  $a_1$  etc. are functions of the six cross sections  $\sigma_{ik}$ . Substituting into (5) the values of these cross sections for hydrogen at 32 kev, we can calculate  $N^-/N^+$  at various gas pressures in the collision chamber and compare the results with our experimental curve  $N^-/N^+ = f(p)$ . Figure 7 shows that the experimental curve and the curve plotted according to Eq. (5) are in good agreement.

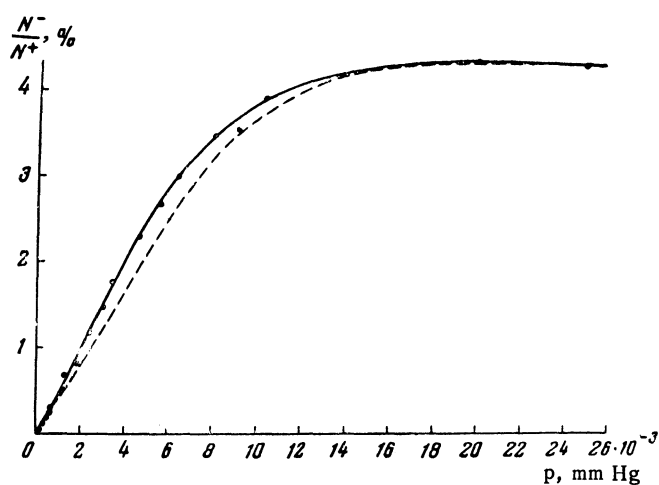


FIG. 7.  $N^-/N^+ = f(p)$ : dashed curve – calculated from Eq. (6); solid curve – experimental.

The comparisons which have been made show that our measurements of  $\sigma_{10}$ ,  $\sigma_{0-1}$ ,  $\sigma_{-11}$ ,  $\sigma_{1-1}$ ,  $\sigma_{01}$  and  $(N^-/N^+)$  do not contain large errors and can therefore be used to calculate the composition of a hydrogen beam in a hydrogen target. For calculating the composition of the beam in inert gases and in  $N_2$  and  $O_2$  together with our measured results for  $\sigma_{01}$ ,  $\sigma_{0-1}$ ,  $\sigma_{-11}$  and  $\sigma_{1-1}$  the values of  $\sigma_{10}$  and  $\sigma_{-10}$  in Refs. 7 and 16 can be used.

Our knowledge of the six cross sections for charge transfers in hydrogen particles colliding with gas particles permits us to compare these cross sections among themselves. The three electron-capture cross sections and the three electron-loss cross sections obey the following inequalities\*

in the investigated energy range:

$$\sigma_{1-1} < \sigma_{0-1} < \sigma_{10}, \quad (6a)$$

$$\sigma_{-11} < \sigma_{01} < \sigma_{-10}. \quad (6b)$$

Conclusions derived from these inequalities are in full agreement with expectations. It follows from (6) that: (1) the cross sections for two-electron processes are smaller than the cross sections for one-electron processes, (2) the cross section for single-electron capture increases with the binding energy of the electron in the resulting particle ( $\sigma_{0-1} < \sigma_{10}$ ), and (3) the cross section for the loss of a single electron decreases with increase of the electron binding energy in the particle which loses the electron ( $\sigma_{01} < \sigma_{-10}$ ).

From the numerical values of the six cross sections which determine the composition of the beam we see that  $\sigma_{10}$  is about two orders greater than  $\sigma_{1-1}$  and  $\sigma_{0-1}$ , and that the latter two cross sections do not differ very much from each other ( $\sigma_{1-1}$  amounts to from 30 to 80% of  $\sigma_{0-1}$ ).  $\sigma_{-10}$  is about one order of magnitude larger than  $\sigma_{-11}$  and  $\sigma_{01}$ , which also do not differ very much ( $\sigma_{-11}$  is from 30 to 70% of  $\sigma_{01}$ ). The ratios of the capture and loss cross sections in the investigated energy interval are characterized by the following numerical relationships:  $\sigma_{1-1}/\sigma_{-11}$  varies between 1 and 30%;  $\sigma_{0-1}/\sigma_{-10}$  is 0.5–2%;  $\sigma_{10}/\sigma_{01}$  for all gases except helium decreases from a magnitude on the order of 10 at the beginning of the range to the order of unity at the end of the range. For helium this ratio varies very little in the energy range under investigation and is close to unity. From the dependence of the ratios  $\sigma_{ik}/\sigma_{ki}$  on the parameter  $\gamma$  ( $\gamma = v_i/v$ , where  $v_i$  is the orbital velocity of the electron in a moving particle and  $v$  is the velocity of the particle) it can be seen that for  $\gamma = 1$   $\sigma_{1-1}/\sigma_{-11}$  and  $\sigma_{0-1}/\sigma_{-10}$  are very far from unity whereas  $\sigma_{10}/\sigma_{01}$  differs very little from unity for  $\gamma = 1$ . Therefore the hypothesis that the electron capture and loss cross sections are equal when the particle velocity equals the orbital velocity of the electron is approximately valid only for  $H_1^0 \rightleftharpoons H_1^+$ , and is not valid for  $H_1^+ \rightleftharpoons H_1^-$  and  $H_1^0 \rightleftharpoons H_1^-$ .

The maxima of the curves  $\sigma_{0-1} = f(E)$  in He, Ne,  $H_2$ ,  $N_2$  and  $O_2$  permit us to estimate the impact parameter for the corresponding processes on the basis of Massey's adiabatic criterion [see Eq. (2) of Ref. 25]. The resonance defect for electron capture by fast atoms  $A + B = A^- + B^+$  can be put into the form

$$\Delta E = S_A - V_B', \quad (7)$$

where  $S_A$  is the electron affinity of particle A

\*There is a single exception for  $\sigma_{-11}$  and  $\sigma_{01}$  at 5 kev in  $O_2$  and  $N_2$ , where  $\sigma_{-11} > \sigma_{01}$ .

and  $V_B^I$  is the first ionization potential of particle B. In the case of molecular gases electron capture by A can occur in two ways:  $A + B_2 = A^- + B_2^+$  and  $A + B_2 = A^- + B^+ + B$ , i.e., in the first instance a slow singly charged molecular ion is formed, while in the second instance this ion is dissociated. In the latter instance the resonance defect is calculated from the formula

$$\Delta E = S_A - (V_{B_2^+} + E_{\text{dis}}), \quad (8)$$

where  $E_{\text{dis}}$  is the dissociation energy of  $B_2^+$ .

The table contains the values of the impact parameter which were computed by means of Massey's adiabatic criterion. The values marked with asterisks refer to cases in which the molecular ion is dissociated. The impact parameter varies very little for different target particles, especially when it is assumed that electron capture in molecular gases is accompanied by the dissociation of a slow molecular ion; the mean impact parameter in this case is 3 Å. The same condition applies to the capture of a single electron<sup>4,7</sup> or two electrons<sup>17,25</sup> by singly charged positive ions; for these processes the mean impact parameter is 8 Å and 1.5 Å, respectively. Thus for the capture of a single electron by an atom, the particles must approach closer than for the capture of a single electron by a positive ion. The particles must approach closest for the capture of two electrons by a positive ion.

Gas	Resonance defect $\Delta E$ (ev)	Maximum		Impact parameter (Å)
		E, (kev)	V, cm/sec	
He	-23.7	20	$2 \cdot 10^8$	3.4
Ne	-20.7	10	$1.4 \cdot 10^8$	2.8
H <sub>2</sub>	-14.7	10.2	$1.4 \cdot 10^8$	4.0
	-17.3*			3.4*
N <sub>2</sub>	-15.1	11	$1.45 \cdot 10^8$	4.0
	-23.8*			2.5*
O <sub>2</sub>	-11.8	8	$1.24 \cdot 10^8$	4.4
	-18.2*			2.8*

The dependence of  $\sigma_{0-1}$  on the electron binding energy in a target atom can be expressed most directly in terms of the resonance defect  $|\Delta E|$  (see Eq. (7)). Figure 8 shows the dependence of  $\sigma_{0-1}$  on  $|\Delta E|$  for H atoms with an energy of 5 kev (curve 1) and 30 kev (curve 2). These points for  $H_1^0 \rightarrow H_1^-$  in inert gases can be connected by smooth curves representing the monotonic reduction of  $\sigma_{0-1}$  as the resonance defect increases. The values for oxygen fit both curves well if it is assumed that electron capture from an oxygen molecule is accompanied by dissociation of the molecular oxygen ion. A point for nitrogen lies on curve 2 if, on the con-

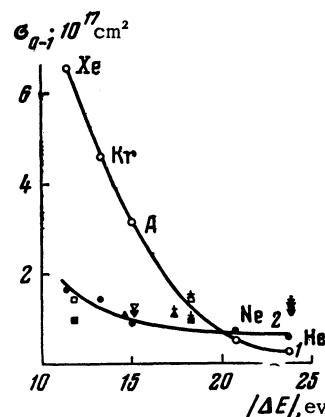


FIG. 8. Resonance defect according to Eq. (7):  $\square, \blacksquare$  - for O<sub>2</sub>;  $\blacktriangle$  - for H<sub>2</sub>;  $\nabla, \blacktriangledown$  - for N<sub>2</sub>. The same symbols with a plus sign above give the resonance defect according to Eq. (8). The solid symbols refer to 30 kev.

trary, it is assumed that the molecular nitrogen ion does not dissociate. The same applies to hydrogen. Values for nitrogen do not lie on curve 1 whether the molecular ion is dissociated or not. There is still insufficient experimental information available for any conclusions to be drawn from the arrangement of values for molecular gases on the curve for  $\sigma_{0-1} = f(|\Delta E|)$  as to which form of the process  $H_1^0 \rightarrow H_1^-$  occurs in a molecular gas.

The observed reduction of  $\sigma_{0-1}$  as the absolute value of the resonance defect increases confirms the conclusion reached regarding the reduction of this cross section as the electron binding energy in a target atom is increased. Figure 8 shows that this relationship is much more pronounced at lower velocities of the hydrogen atom.

A consideration of the curves for  $\sigma_{01} = f(E)$  shows that it is not correct to postulate the same impact parameter for the process  $H_1^0 \rightarrow H_1^+$  in all of the gases investigated here, because a resonance defect equal in absolute magnitude to the ionization potential of the hydrogen atom would be the same for all gases, so that the maximum cross section would be observed at the same energy for the various gases. Figures 3 and 4 show clearly that this is not the case. It is possible that the adiabatic postulate cannot be applied to electron loss by fast atoms as it can for electron loss by negative ions. An analysis of the experimental cross sections for electron capture and loss by hydrogen particles suggests that Massey's adiabatic postulate is in good agreement with electron capture processes but cannot be applied to electron loss. Any decision as to the applicability of the adiabatic postulate to electron capture and loss by fast atoms will have a firmer basis after measurements of  $\sigma_{0-1}$

and  $\sigma_{01}$  at low energies where the slow collision condition  $a|\Delta E|/h\nu \gg 1$  will be fulfilled. However, for measurements in this energy range the sensitivity of our experimental procedure will have to be considerably increased.

We wish to thank N. I. Bliznetsov and A. G. Shevchenko for preparing the vacuum thermocouples which were used in the present work. The authors also consider it a pleasant duty to thank Prof. A. K. Val' ter for his continued interest.

<sup>1</sup>J. P. Keene, *Phil. Mag.* **40**, 369 (1949).

<sup>2</sup>F. L. Ribe, *Phys. Rev.* **83**, 1217 (1951).

<sup>3</sup>H. Kanner, *Phys. Rev.* **84**, 1211 (1951).

<sup>4</sup>J. B. Hasted, *Proc. Roy. Soc. (London)* **A212**, 235 (1952).

<sup>5</sup>A. C. Whittier, *Can. J. Phys.* **32**, 275 (1954).

<sup>6</sup>Fogel', Krupnik, and Safronov, *J. Exptl. Theoret. Phys. (U.S.S.R.)* **28**, 589 (1955), *Soviet Phys. JETP* **1**, 415 (1955).

<sup>7</sup>J. B. H. Stedeford and J. B. Hasted, *Proc. Roy. Soc. (London)* **A227**, 466 (1955).

<sup>8</sup>de Heer, Huizenga, and Kistemaker, *Physica* **23**, 181 (1957).

<sup>9</sup>D. R. Bates and A. Dalgarno, *Proc. Phys. Soc. (London)* **A65**, 919 (1952); **A66**, 972 (1953).

<sup>10</sup>A. Dalgarno and H. N. Yaday, *Proc. Phys. Soc. (London)* **A66**, 173 (1953).

<sup>11</sup>J. D. Jackson and H. Schiff, *Phys. Rev.* **89**, 359 (1953).

<sup>12</sup>D. R. Bates and G. W. Griffing, *Proc. Phys. Soc. (London)* **A66**, 961 (1953).

<sup>13</sup>Bransden, Dalgarno, and King, *Proc. Roy. Soc. (London)* **A67**, 1075 (1954).

<sup>14</sup>T. Pradhan, *Phys. Rev.* **105**, 1250 (1957).

<sup>15</sup>J. H. Montague, *Phys. Rev.* **81**, 1026 (1951).

<sup>16</sup>P. M. Stier and C. F. Barnett, *Phys. Rev.* **103**, 896 (1956).

<sup>17</sup>Ia. M. Fogel' and R. V. Mitin, *J. Exptl. Theoret. Phys. (U.S.S.R.)* **30**, 450 (1956), *Soviet Phys. JETP* **3**, 334 (1956).

<sup>18</sup>Fogel', Ankudinov, and Slabospitskii, *J. Exptl. Theoret. Phys. (U.S.S.R.)* **32**, 453 (1957), *Soviet Phys. JETP* **5**, 382 (1957).

<sup>19</sup>Fogel', Krupnik, and Ankudinov, *J. Tech. Phys. (U.S.S.R.)* **26**, 1208 (1956), *Soviet Phys. JTP* **1**, 1181 (1956).

<sup>20</sup>J. A. Weinmann and J. R. Cameron, *Rev. Sci. Instr.* **27**, 288 (1956).

<sup>21</sup>Fogel', Krupnik, Koval', and Slabospitskii, *J. Tech. Phys. (U.S.S.R.)* **27**, 988 (1957), *Soviet Phys. JTP* **2**, 902 (1957).

<sup>22</sup>A. Dalgarno and G. W. Griffing, *Proc. Roy. Soc. (London)* **A232**, 423 (1955).

<sup>23</sup>O. Reifenschweiler, *Ann. Phys.* **14**, 33 (1954).

<sup>24</sup>Ia. M. Fogel' and L. I. Krupnik, *J. Exptl. Theoret. Phys. (U.S.S.R.)* **29**, 209 (1955), *Soviet Phys. JETP* **2**, 252 (1956).

<sup>25</sup>Fogel', Mitin, and Koval', *J. Exptl. Theoret. Phys. (U.S.S.R.)* **31**, 397 (1956), *Soviet Phys. JETP* **4**, 359 (1957).

<sup>26</sup>Fogel, Lisochkin, and Stepanova, *J. Tech. Phys. (U.S.S.R.)* **25**, 1944 (1955).

<sup>27</sup>H. Bartels, *Ann. Phys.* **13**, 373 (1932).

<sup>28</sup>D. R. Bates and G. W. Griffing, *Proc. Phys. Soc. (London)* **A68**, 90 (1955).

<sup>29</sup>D. R. Bates and A. Williams, *Proc. Phys. Soc. (London)* **A70**, 306 (1957).

<sup>30</sup>L. D. Jackson, *Proc. Phys. Soc. (London)* **A70**, 26, (1957).

Translated by I. Emin

115